Cell Systems

Report

Encoding Membrane-Potential-Based Memory within a Microbial Community

Graphical Abstract

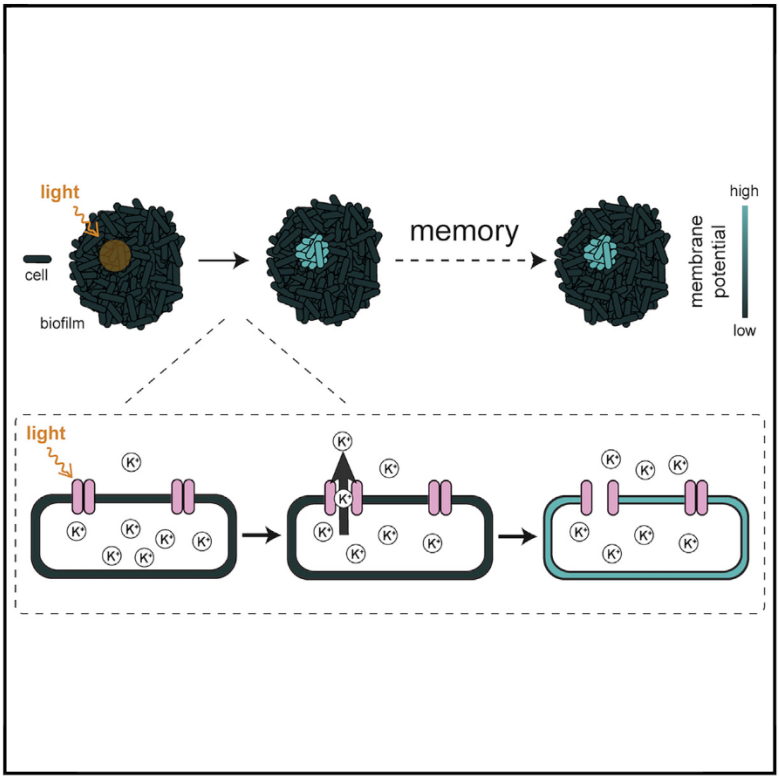

Authors

Chih-Yu Yang, Maja Bialecka-Fornal, Colleen Weatherwax, ..., Jintao Liu, Jordi Garcia-Ojalvo, Gürol M. Süel

Correspondence

gsuel@ucsd.edu

In Brief

We find that transient light exposure induces persistent and robust membrane potential-encoded memory in bacteria. Similarities between this memory and neuronal memory imply that processes thought to be neuron specific might have early roots in bacterial systems. This discovery could promote biological computation through imprinting of complex spatial memory patterns in biofilms.

Highlights

- Bacteria form membrane-potential-based memory, reminiscent of neurons
- Bacterial memory is formed through a light-induced change to potassium channels
- As predicted by a Hodgkin-Huxley model, memory is robust to ionic perturbations
- Complex memory patterns can be encoded in a biofilm at the single-cell level

Yang et al., 2020, Cell Systems *10*, 417–423
May 20, 2020
https://doi.org/10.1016/j.cels.2020.04.002

CellPress

Cell Systems

CellPress

Report

Encoding Membrane-Potential-Based Memory within a Microbial Community

Chih-Yu Yang,[1,7] Maja Bialecka-Fornal,[1,7] Colleen Weatherwax,[1] Joseph W. Larkin,[1] Arthur Prindle,[1,2] Jintao Liu,[1,3] Jordi Garcia-Ojalvo,[4] and Gürol M. Süel[1,5,6,8,*]

[1]Division of Biological Sciences, University of California, San Diego, Pacific Hall Room 2225B, Mail Code 0347, 9500 Gilman Drive, La Jolla, CA 92093, USA

[2]Department of Biochemistry and Molecular Genetics, Feinberg School of Medicine, Northwestern University, Chicago, IL 60611, USA

[3]Center for Infectious Diseases Research and Tsinghua-Peking Center for Life Sciences, School of Medicine, Tsinghua University, Beijing 100084, People's Republic of China

[4]Department of Experimental and Health Sciences, Universitat Pompeu Fabra, Barcelona Biomedical Research Park, Barcelona 08003, Spain

[5]San Diego Center for Systems Biology, University of California, San Diego, La Jolla, CA 92093, USA

[6]Center for Microbiome Innovation, University of California, San Diego, La Jolla, CA 92093-0380, USA

[7]These authors contributed equally

[8]Lead Contact

*Correspondence: gsuel@ucsd.edu

https://doi.org/10.1016/j.cels.2020.04.002

SUMMARY

Cellular membrane potential plays a key role in the formation and retrieval of memories in the metazoan brain, but it remains unclear whether such memory can also be encoded in simpler organisms like bacteria. Here, we show that single-cell-level memory patterns can be imprinted in bacterial biofilms by light-induced changes in the membrane potential. We demonstrate that transient optical perturbations generate a persistent and robust potassium-channel-mediated change in the membrane potential of bacteria within the biofilm. The light-exposed cells respond in an anti-phase manner, relative to unexposed cells, to both natural and induced oscillations in extracellular ion concentrations. This anti-phase response, which persists for hours following the transient optical stimulus, enables a direct single-cell resolution visualization of spatial memory patterns within the biofilm. The ability to encode robust and persistent membrane-potential-based memory patterns could enable computations within prokaryotic communities and suggests a parallel between neurons and bacteria.

INTRODUCTION

Recent studies by multiple groups have revealed surprising functional roles of ion-channel-mediated signaling (action potentials) in bacteria and their biofilm communities (Bruni et al., 2017; Humphries et al., 2017; Liu et al., 2017; Prindle et al., 2015; Sirec et al., 2019; Stratford et al., 2019). Interestingly, it has been shown that bacteria undergoing membrane potential spikes are likely to experience them in the future (Larkin et al., 2018), suggesting that bacteria may have the ability to store information about their past membrane potential state. This finding suggests the possibility that membrane-potential-based memory could be encoded in a bacterial system. Encoding memory has been a sustained focus of systems and synthetic biology. The majority of synthetic biology approaches capable of encoding memory in cells, including simple systems, such as bacteria, rely on manipulation of DNA sequences (Ajo-Franklin et al., 2007; Farzadfard and Lu, 2014; Gardner et al., 2000; Ho and Bennett, 2018). This is a logical and powerful approach, since organisms naturally use DNA to store information, and changes in DNA sequences are typically persistent and robust. On the other hand, physiological memory is commonly associated with neurons in the brain, which utilize cellular membrane potential modulation rather than genetic changes (Axmacher et al., 2006; Hasselmo and Brandon, 2008; Shim et al., 2018; Sweatt, 2016). In particular, membrane-potential-based memory in neuronal systems can arise from persistent protein modifications that can, for example, alter the flux of ions through channels (Sweatt, 2016; Tsien, 2013). Encoding such memory at the level of the membrane potential could have unique advantages within the context of synthetic biology, as it would not require the introduction of positive feedback loops via ectopic components, such as engineered enzymes, into cells. However, synthetic biology studies have so far not utilized the membrane potential, despite it being a ubiquitous feature in all living cells. Here, we demonstrate that it is possible to encode memory within a bacterial biofilm community through a long-lasting change in the membrane potential of individual bacteria.

RESULTS

To induce a change in the membrane potential of *B. subtilis* cells, we asked whether we could alter the flux through ion channels. It has been previously reported that blue light

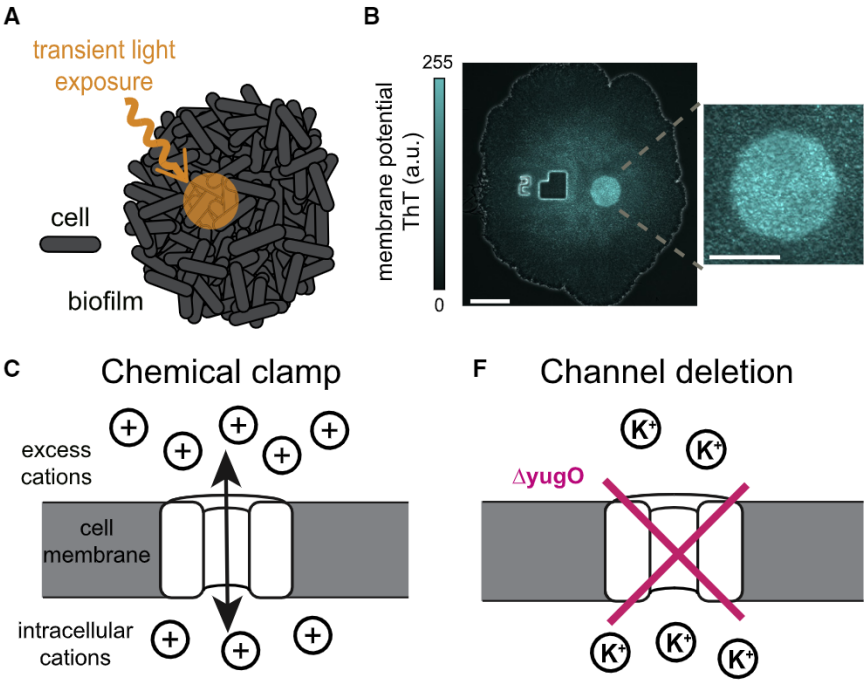

Figure 1. Light Stimulation Alters Membrane Potential in *B. subtilis* Biofilms

(A) Cartoon showing local light stimulation in a biofilm.

(B) Left: snapshot of a biofilm showing that local light stimulation causes the hyperpolarization of membrane potential. Phase contrast is overlaid with fluorescence of ThT (cyan), the Nernstian membrane potential reporter. Scale bar, 100 μm. Right: the magnified light-exposed region. Scale bars, 50 μm.

(C) Cartoon showing a chemical clamp. Excess of specific cations reduces the outward chemical gradient.

(D) Snapshots in ThT fluorescence (cyan) showing biofilms before (left column) and 40 min after light exposure (right column) in the presence of regular media (MSgg, STAR Methods; top row), excess potassium (regular media + 150 mM KCl; middle row), and excess sodium (regular media + 150 mM NaCl; bottom row). Scale bar, 50 μm.

(E) Bar plot showing the percent change of ThT intensity 40 min after light exposure in regular media, excess potassium, and excess sodium (mean ± SD, n = 10 exposed regions).

(F) Cartoon showing lack of potassium flux in YugO deletion strain.

(G) Snapshots in ThT fluorescence (cyan), showing wild-type (top row) and *ΔyugO* (bottom row) biofilms before (left column) and 40 min after exposure to blue light (right column). Scale bar, 50 μm.

(H) Bar plot showing the percent change of ThT intensity 40 min after light exposure of wild-type and *ΔyugO* biofilms (mean ± SD, n = 15 exposed regions).

See also Figures S1 and S2.

increases the flux through cation channels (Nagel et al., 2003; Suh et al., 2000). Therefore, we tested whether exposure of bacterial cells to blue light would have a similar effect (Figure 1A). Indeed, we find that a short (5 s) blue-light (438 nm) exposure hyperpolarizes the membrane potential of *B. subtilis* cells within biofilm communities. Specifically, we observe an increase in the intensity of the Nernstian membrane potential reporter, thioflavin-T (ThT) (Prindle et al., 2015), for light-exposed cells (Figure 1B; STAR Methods). This membrane hyperpolarization is specific to blue light and, as expected, increases with higher exposure intensity (Figures S1A and S1B). We confirmed that the observed ThT signal was not an artifact caused by cell death or a general increase in cell permeability, by using either propidium iodide (PI), or Sytox, which are two standard cell permeability markers, as a control (Figure S1C). Independently, we further confirmed that the light-induced change in the membrane potential was not a terminal response caused by lethal damage, by testing whether light-exposed cells could respond to a metabolic stimulus. Specifically, we show that addition of glutamine, which provides nitrogen for metabolism and protein synthesis, enables the hyperpolarized cells to return to their resting potential (Figure S1D). Additional controls verified that the membrane potential indicator dye, ThT, does not play an active role in the observed membrane hyperpolarization, and that the commonly used membrane potential quenching agent, carbonyl cyanide m-chlorophenyl hydrazone (CCCP), also quenches the observed

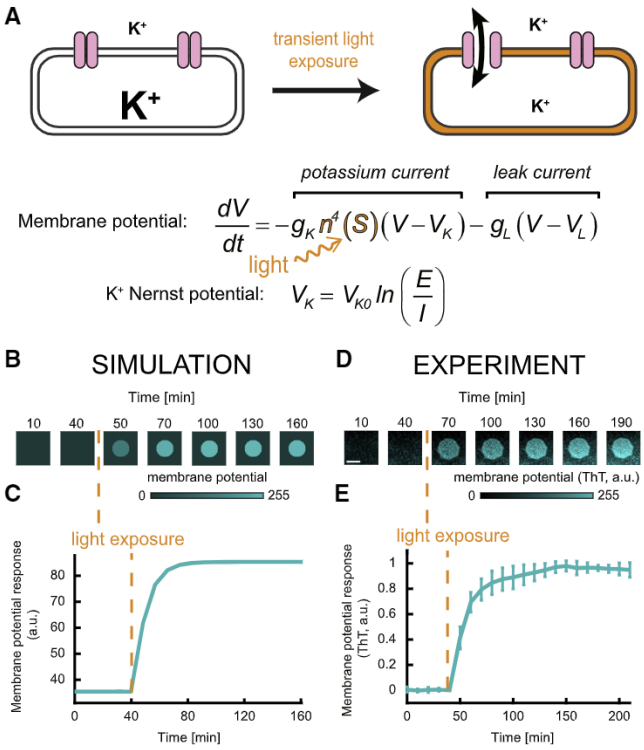

Figure 2. Model Prediction and Experimental Validation of the Persistence of Light-Induced Membrane Potential Change

(A) Cartoon (top) and equations (bottom) of the proposed model. The cartoon is a schematic of potassium channel (pink) gating and potassium flux before (left) and after (right) transient light exposure. The equations describe membrane potential change and Nernst potential for potassium (STAR Methods). The orange wavy arrow pointing to the orange colored n(S) in the equation shows that light increases and fixes n, the fraction of open potassium channels, and eliminates the dependence of n on S (metabolic stress).

(B) Simulated filmstrip showing change in membrane potential in an exposed region of the biofilm over time. Transient light exposure at 40 min (orange dashed line).

(C) Model-predicted membrane potential dynamics of the exposed region of the biofilm, corresponding to data shown in (B). Transient light exposure at 40 min (orange dashed line).

(D) Filmstrip in ThT fluorescence (cyan) showing the change of ThT intensity in an exposed region of a biofilm over time. The experiments were conducted in regular media (MSgg). Scale bar, 50 μm.

(E) Membrane potential (ThT) dynamics of the exposed region of a biofilm in experiments (mean ± SD, n = 5 exposed regions). Light exposure at 40 min is marked with orange dashed line.

See also Figure S3.

light response (Figures S1E, S1F, S2A, and S2B). Together, these data indicate that blue-light exposure modifies, in a non-lethal manner, the membrane potential of bacterial cells within a biofilm community.

Next, we investigated whether the observed change in membrane potential is indeed due to changes in flux through ion channels, which are highly selective for specific ion species. The simplest explanation for the observed hyperpolarization is that positive ions were released from the cell through ion channels. To test whether this is the case, we applied a chemical clamp to cells by increasing the extracellular concentration of specific cations to cancel the outward chemical gradient for cations (Figure 1C). We stimulated with light in the presence of excess sodium or potassium (the two key cations involved in determining the membrane potential of living cells) to see if the chemical clamp prevented the hyperpolarization of light-exposed cells. In the presence of excess sodium, the stimulated area shows an increase in ThT intensity comparable with regular growth media (Figures 1D and 1E). However, in the presence of excess potassium, we did not observe such hyperpolarization (Figures 1D and 1E). We ruled out an osmotic effect of potassium salt addition by confirming that addition of sorbitol, an uncharged osmolyte, has no effect on the membrane potential response (Figures S2C and S2D). These data show that an increased concentration of extracellular potassium specifically prevents hyperpolarization of light-exposed cells. Therefore, light-induced hyperpolarization is potassium selective, a finding that suggests the involvement of a potassium-selective ion channel.

To directly confirm that light alters flux through the potassium channel, we genetically deleted YugO, the only known potassium channel in *B. subtilis* (Figure 1F; STAR Methods) (Lundberg et al., 2013). The observed cellular hyperpolarization implies that light promotes an efflux of potassium ions through YugO channels. Therefore, bacteria lacking the YugO channel should be deficient in their ability to release potassium ions (Prindle et al., 2015) and thus should not hyperpolarize upon light stimulation. Indeed, the YugO deletion bacterial strain does not exhibit a noticeable membrane potential change upon light exposure (Figures 1G and 1H). From these multiple lines of evidence, we conclude that local exposure to blue light hyperpolarizes the membrane potential by increasing the flux of potassium ions through the *B. subtilis* YugO channel.

To gain a deeper understanding of how manipulating the flux through the potassium channel affects the membrane potential and whether these changes can be persistent and robust, we constructed a phenomenological model based on the Hodgkin-Huxley mathematical framework (Figure 2A; STAR Methods). Our model assumes that the dynamics of membrane potential in a single cell depends on the flux of potassium through ion channels. The intracellular and extracellular potassium concentrations are interdependent and define the direction of potassium flux upon channel opening, based on the Nernst equation. Consistent with previous reports, the model also assumes that the gating of the channels is controlled by cell stress that depends on changes in membrane potential (Prindle et al., 2015). We simulate light exposure by assuming that it increases and fixes the variable (n), which determines the fraction of ion channels that are in the open (conducting) configuration. We can thus utilize this Hodgkin-Huxley-based model to simulate membrane potential responses to light stimulation and investigate the persistence and robustness of these responses.

First, we tested whether this locally and transiently induced change in cell polarization persists over time. The model indeed predicts an increased membrane potential in response to light exposure that reaches a steady state within minutes and persists indefinitely (Figures 2B and 2C). This sustained hyperpolarization results from the partial permanent opening of potassium channels that is assumed to be caused by transient light stimulation in exposed cells. To test this prediction experimentally, we exposed a region of biofilm to blue light and observed that the

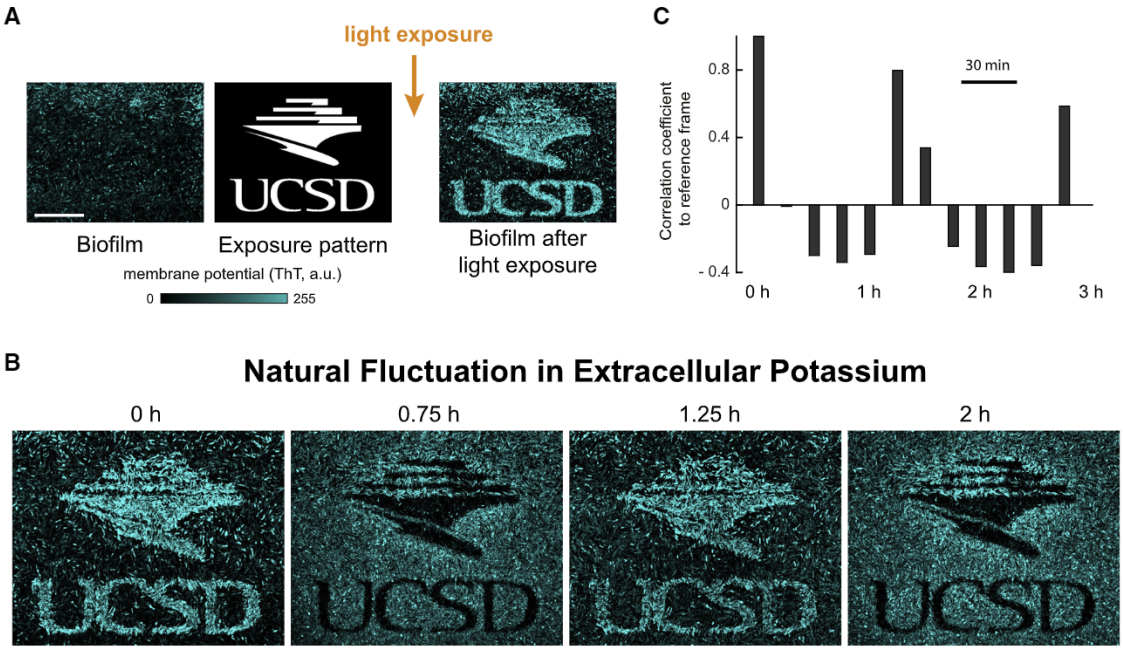

Figure 3. Persistence and Robustness of a Light-Encoded Pattern in a Biofilm under Natural Fluctuations of Extracellular Potassium

(A) Schematic showing light encoding of a complex pattern onto a biofilm. Scale bar, 40 μm.

(B) Filmstrip indicating the membrane potential (ThT) dynamics of cells within the biofilm region from (A) during natural fluctuations in extracellular potassium. We note that the natural fluctuations of extracellular potassium are not induced by light but rather are global oscillations within the biofilm as reported in Liu et al. (2015). The experiments were conducted in regular media (MSgg).

(C) Bar plot showing the correlation coefficient of ThT intensity between pixel data at t = 0 h and data from progressive time points. Scale bar, 30 min.

exposed area is distinguishable from the rest of the biofilm within a minute (Figure S3). As in the simulation, ThT intensity reached its maximum within minutes after light stimulation and remained at a steady state throughout the observation time of over 3 h (Figures 2D and 2E; Video S1). This result shows that the memory of a transiently imprinted membrane potential pattern within a *B. subtilis* biofilm persists for hours.

We next asked whether light-encoded memory can persist in a dynamical, growing biofilm undergoing natural changes in extracellular potassium concentrations that directly affect the cellular membrane potential. In contrast to the growth conditions used in the experiments of Figure 2, sufficiently large biofilms can experience glutamate starvation, which triggers periodic oscillations in extracellular potassium concentration within the biofilm. These oscillations, mediated by potassium ion channels, enable long-range communication to alleviate starvation (Liu et al., 2015; Prindle et al., 2015). We thus tested whether an intricate spatial pattern encoded at the level of the membrane potential is also robust against such naturally occurring changes in extracellular ion concentrations (Figure 3A; STAR Methods). We find that the spatial memory pattern indeed persists for hours despite fluctuations in extracellular ion concentrations. Interestingly, the membrane potential pattern exhibits an anti-correlated (anti-phase) behavior with the rest of the biofilm (Figure 3B and Video S2). In other words, the light-exposed cells transition back and forth from being hyperpolarized to becoming depolarized, relative to the rest of the biofilm. This results in striking visual patterns over time, where light-exposed cells are collectively hyperpolarized or depolarized, relative to the rest of the biofilm. Concurrently, the spatial pattern periodically alternates between being either positively or negatively correlated with its initial reference frame (Figure 3C). These data show that even highly intricate spatial patterns encoded at the level of the membrane potential are not only robust to naturally occurring changes in extracellular potassium concentrations perturbations, but the patterns remain visually distinguishable from the rest of the biofilm over several hours.

We further utilized our mathematical model to establish whether the observed periodic alternation in the membrane potential between hyperpolarization and depolarization was caused by changes in extracellular potassium concentrations within the biofilm (Figure 4A; STAR Methods). We note that cells unexposed to light are able to control intracellular potassium levels through ion channel gating. Specifically, under excess potassium, unexposed cells actively respond by opening their potassium channels and releasing intracellular ions (Prindle et al., 2015). In this way, light-unexposed cells hyperpolarize in response to elevated extracellular potassium levels. On the other hand, our findings suggest that light exposure causes a long-term alteration in the flux through potassium channels (Figures 1D–1H). Consequently, our model predicts that high extracellular potassium levels result in the influx of potassium into light-exposed cells, leading to their depolarization. To determine the validity of this process in a more rigorous manner, we simulated the dynamics of membrane potential changes under periodic alternation of high (150 mM K^+) and regular (8 mM K^+) extracellular potassium concentrations. The simulation results show that two types of cells (light exposed and unexposed) indeed

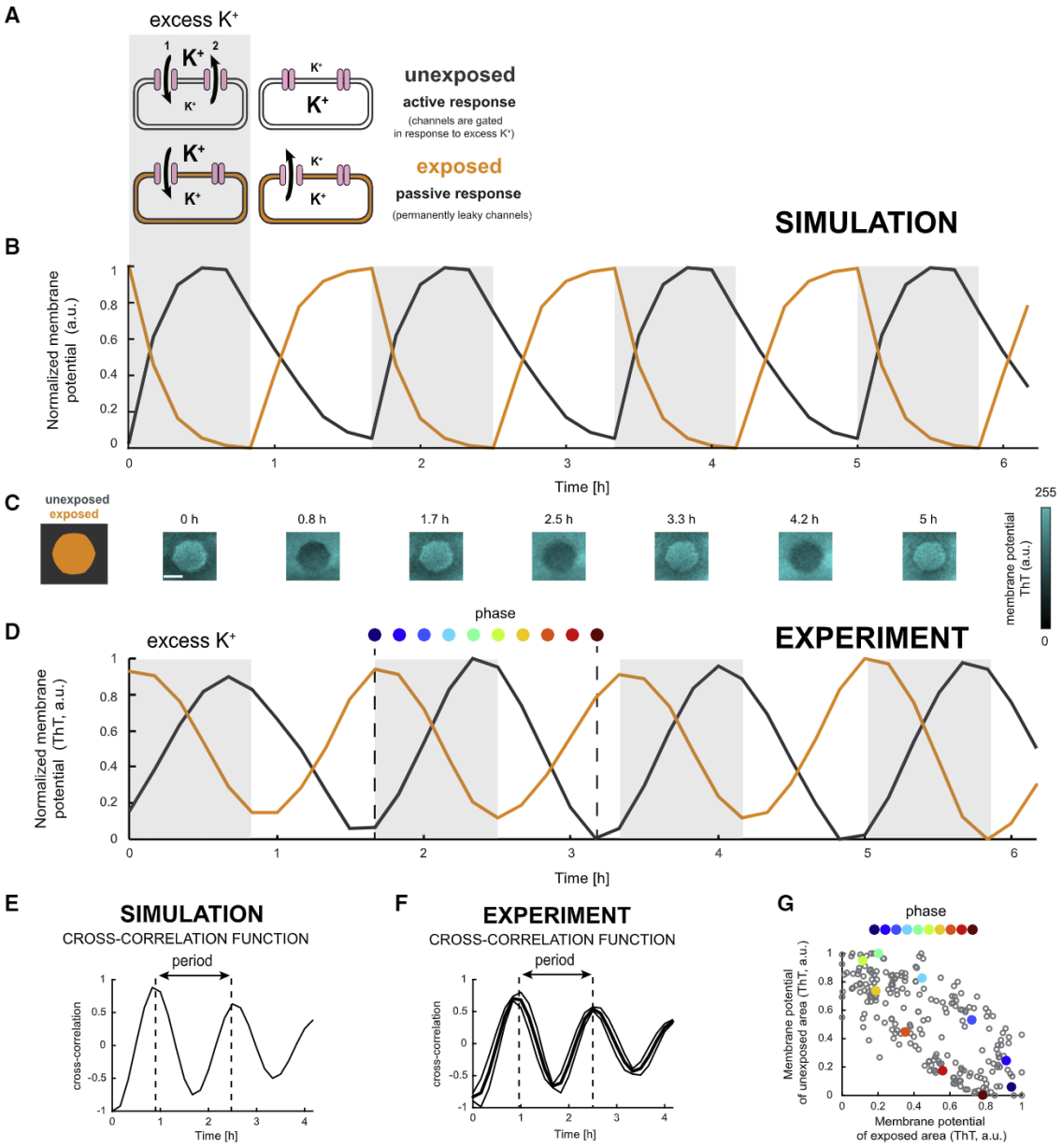

Figure 4. Membrane Potential Dynamics under Extracellular Potassium Fluctuations

(A) Cartoon showing the gating of potassium channels (pink) and potassium flux in unexposed (black, top row) and exposed (orange, bottom row) cells under high extracellular potassium (left column, light gray shaded area) and regular media (right column) conditions. In unexposed cells, uptake of potassium (1) is followed by outflux (2). The font size of potassium (K+) indicates the relative potassium concentration.

(B) Model-predicted membrane potential dynamics of unexposed (black) and exposed (orange) cells under alternating concentrations of high (light gray shaded area) and regular extracellular potassium.

(C) Left: diagram showing unexposed (black) and exposed (orange) regions of the biofilm. Right: filmstrip in ThT fluorescence (cyan), showing membrane potential (ThT) dynamics during alternating concentrations of high (regular media + 150 mM KCl) and regular extracellular potassium (regular media). Scale bar, 50 μm.

(D) Membrane potential dynamics (ThT) of unexposed (black) and exposed (orange) regions of the biofilm under alternating concentrations of high (light gray shaded area) and regular extracellular potassium, corresponding to the filmstrip in (C). Dashed lines outline one period. Colored dots represent individual time points.

(E) Cross-correlation for the two simulated membrane potential data series in (B). Dashed lines show one period.

(F) Average cross-correlation (central black line) of membrane potential data from exposed and unexposed regions during alternating concentrations of high and regular extracellular potassium (n = 5 exposed regions). Thinner black lines represent mean ± SEM.

(G) Scatter plot showing negative correlation of membrane potential (ThT) between unexposed and exposed regions of the biofilm (n = 22 oscillatory periods). Colored dots correspond to individual time points shown in (D).

See also Figure S4.

respond oppositely to changes in extracellular potassium. Specifically, we assume that light-exposed cells have a fraction of ion channels that are permanently in the conducting state. Consequently, the membrane potential of exposed cells will passively follow extracellular potassium levels: decreasing under excess potassium (the cell becomes less negative) but recovering right after switching to regular (low) potassium concentration. Conversely, unexposed cells retain control over their potassium ion channels. These cells can respond actively to excess external potassium by dynamically controlling their potassium channels and becoming hyperpolarized when the cation is in excess (Figure 4B). This results in an approximately anti-phase behavior between light-exposed and -unexposed cells during changes in extracellular potassium, making exposed cells clearly distinguishable from unexposed cells.

To validate these simulation results, we utilized the microfluidics capability of our experimental setup to artificially alternate the extracellular potassium concentration periodically between high (150 mM K^+) and regular (8 mM K^+) levels during the course of the experiment (STAR Methods). We note that we conducted this experiment using biofilms that did not undergo natural fluctuations in extracellular potassium (Prindle et al., 2015). Consistent with our mathematical model, we observed that the exposed and unexposed biofilm regions responded oppositely to controlled changes in extracellular potassium concentrations (Figures 4C, 4D, and S4A; Video S3). Thus, in both simulations and experiments, the dynamics of membrane potential between exposed and unexposed cells exhibit an anti-phase behavior during changes in extracellular potassium (Figures 4E–4G). Specifically, the cross-correlation function is anti-correlated at zero lag time and maximally correlated at 50 min lag time, which corresponds to half of the pre-determined period of alternating potassium conditions (Figures 4E and 4F). Furthermore, consistent with the assumption that light exposure increases the fraction of open channels, we find that the exposed region exhibits a higher ThT amplitude compared with the unexposed region, in both simulations and experiments (Figures S4B and S4C). These results confirm the mathematical predictions, and thus demonstrate that the observed anti-phase behavior of the encoded memory pattern with respect to the rest of the biofilm is indeed due to the optically induced difference in the flux of potassium ions in light-exposed cells. These results also demonstrate the striking robustness of the spatial memory pattern during changes in extracellular conditions that directly affect the membrane potential.

DISCUSSION

In summary, our results show that memory can be encoded at the level of the membrane potential of bacteria residing within biofilm communities. The ability to retain memory of membrane potential changes has direct relevance to naturally occurring electrical signaling processes in *B. subtilis* biofilms since both processes are mediated by the YugO potassium ion channel. While in this study we utilized blue light as an optical tool to precisely stimulate a membrane potential response in a subset of cells within a biofilm, membrane potential heterogeneity among cells is known to naturally arise in biofilms (Larkin et al., 2018). Therefore, the ability of a subset of bacteria to retain a membrane-potential-based memory described here may explain how subpopulations of cells within biofilms that are naturally electrically active are able to retain such activity in future signaling events (Larkin et al., 2018). Specifically, our work directly shows that membrane potential heterogeneity within biofilms can persist over time and be robust to extracellular perturbations. According to our model, the cells that repeatedly participate in electrical signaling could have a fraction of ion channels that remain in the open (conducting) state. From a broader perspective, the ability of bacteria to retain memory encoded at the level of the membrane potential is somewhat reminiscent of neurons, where past membrane potential activity can determine future events (Sweatt, 2016). Similar to neurons, the memory described here in bacteria does not arise from positive feedback but rather from enduring modifications at the protein level, which in turn alters the response of cells to external ionic inputs. The persistence of modified proteins may be further aided by the fact that, similar to neurons in the brain, bacteria within biofilms predominantly reside in a non-replicating state. It is intriguing to find conceptual similarities among such evolutionarily distant biological systems. The membrane potential is as ancient of a biological feature as the genetic code itself, and it may thus be possible that the highly evolved and specialized processers in neurons have some early roots in much simpler bacterial systems. Additionally, our results also have implications from an applied perspective, in the context of biological computing. Using living tissues to perform computations requires a reliable way to encode information into the tissue. Our study shows that optical perturbation of ion channels can fulfill this role, potentially leading to the ability to perform more complex computations. The fact that light-exposed and -unexposed cells respond to external perturbations in an anti-phase manner allows us to produce a clear signal that is either "on" or "off," as in traditional digital memory. It may thus be possible to imprint synthetic circuits in bacterial biofilms, by activating different kinds of computations in separate areas of the biofilm, through the combined modulation of the electrical response of bacteria by light and chemicals such as glutamine. Overall, our work is likely to inspire new membrane-potential-based approaches in synthetic biology and provide a bacterial paradigm for memory-capable biological systems.

STAR★METHODS

Detailed methods are provided in the online version of this paper and include the following:

- KEY RESOURCES TABLE
- RESOURCE AVAILABILITY
  - Lead Contact
  - Materials Availability
  - Data and Code Availability
- EXPERIMENTAL MODEL AND SUBJECT DETAILS
  - Bacterial Strains
  - Growth Conditions
- METHOD DETAILS
  - Data Analysis
  - Experimental Reproducibility
  - Model Equations and Description

SUPPLEMENTAL INFORMATION

Supplemental Information can be found online at https://doi.org/10.1016/j.cels.2020.04.002.

ACKNOWLEDGMENTS

We thank Leticia Galera-Laporta, Dong-yeon D. Lee, and Kaito Kikuchi for useful discussions; G.M.S. acknowledges support for this research from the National Institute of General Medical Sciences (grant R01 GM121888 to G.M.S.) and the Howard Hughes Medical Institute-Simons Foundation Faculty Scholars program. J.G.-O. acknowledges support from the Spanish Ministry of Science, Innovation and Universities and FEDER (project PGC2018-101251-B-I00 and "'Maria de Maeztu" Programme for Units of Excellence in R\&D, grant CEX2018-000792-M), and from the Generalitat de Catalunya (ICREA Academia programme).

AUTHOR CONTRIBUTIONS

G.M.S., M.B.-F., C.-Y.Y., A.P., J.L., and J.G.-O. designed the research. M.B.-F., C.-Y.Y., A.P., and J.L. performed the experiments. G.M.S., C.W., and J.G.-O. performed the mathematical modeling. M.B.-F, C.-Y.Y., C.W., and J.W.L. performed the data analysis. G.M.S., M.B.-F., C.-Y.Y., C.W., and J.G.-O. wrote the manuscript. All authors discussed the manuscript.

DECLARATION OF INTERESTS

The authors declare no competing interests.

Received: December 16, 2019
Revised: February 13, 2020
Accepted: April 2, 2020
Published: April 27, 2020

REFERENCES

Ajo-Franklin, C.M., Drubin, D.A., Eskin, J.A., Gee, E.P.S., Landgraf, D., Phillips, I., and Silver, P.A. (2007). Rational design of memory in eukaryotic cells. Genes Dev *21*, 2271–2276.

Axmacher, N., Mormann, F., Fernández, G., Elger, C.E., and Fell, J. (2006). Memory formation by neuronal synchronization. Brain Res. Rev. *52*, 170–182.

Bruni, G.N., Weekley, R.A., Dodd, B.J.T., and Kralj, J.M. (2017). Voltage-gated calcium flux mediates *Escherichia coli* mechanosensation. Proc. Natl. Acad. Sci. USA *114*, 9445–9450.

Farzadfard, F., and Lu, T.K. (2014). Synthetic biology. Genomically encoded analog memory with precise in vivo DNA writing in living cell populations. Science *346*, 1256272.

Gardner, T.S., Cantor, C.R., and Collins, J.J. (2000). Construction of a genetic toggle switch in *Escherichia coli*. Nature *403*, 339–342.

Hasselmo, M.E., and Brandon, M.P. (2008). Linking cellular mechanisms to behavior: entorhinal persistent spiking and membrane potential oscillations may underlie path integration, grid cell firing, and episodic memory. Neural Plast *2008*, 658323.

Ho, J.M.L., and Bennett, M.R. (2018). Improved memory devices for synthetic cells. Science *360*, 150–151.

Humphries, J., Xiong, L., Liu, J., Prindle, A., Yuan, F., Arjes, H.A., Tsimring, L., and Süel, G.M. (2017). Species-independent attraction to biofilms through electrical signaling. Cell *168*, 200–209.e12.

Irnov, I., and Winkler, W.C. (2010). A regulatory RNA required for antitermination of biofilm and capsular polysaccharide operons in *Bacillales*. Mol. Microbiol. *76*, 559–575.

Larkin, J.W., Zhai, X., Kikuchi, K., Redford, S.E., Prindle, A., Liu, J., Greenfield, S., Walczak, A.M., Garcia-Ojalvo, J., Mugler, A., and Süel, G.M. (2018). Signal percolation within a bacterial community. Cell Syst *7*, 137–145.e3.

Liu, J., Martinez-Corral, R., Prindle, A., Lee, D.D., Larkin, J., Gabalda-Sagarra, M., Garcia-Ojalvo, J., and Süel, G.M. (2017). Coupling between distant biofilms and emergence of nutrient time-sharing. Science *356*, 638–642.

Liu, J., Prindle, A., Humphries, J., Gabalda-Sagarra, M., Asally, M., Lee, D.Y.D., Ly, S., Garcia-Ojalvo, J., and Süel, G.M. (2015). Metabolic co-dependence gives rise to collective oscillations within biofilms. Nature *523*, 550–554.

Lundberg, M.E., Becker, E.C., and Choe, S. (2013). MstX and a putative potassium channel facilitate biofilm formation in *Bacillus subtilis*. PLoS One *8*, e60993.

Martinez-Corral, R., Liu, J., Prindle, A., Süel, G.M., and Garcia-Ojalvo, J. (2019). Metabolic basis of brain-like electrical signalling in bacterial communities. Philos. Trans. R. Soc. Lond., B, Biol. Sci. *374*, 20180382.

Nagel, G., Szellas, T., Huhn, W., Kateriya, S., Adeishvili, N., Berthold, P., Ollig, D., Hegemann, P., and Bamberg, E. (2003). Channelrhodopsin-2, a directly light-gated cation-selective membrane channel. Proc. Natl. Acad. Sci. USA *100*, 13940–13945.

Prindle, A., Liu, J., Asally, M., Ly, S., Garcia-Ojalvo, J., and Süel, G.M. (2015). Ion channels enable electrical communication in bacterial communities. Nature *527*, 59–63.

Schindelin, J., Arganda-Carreras, I., Frise, E., Kaynig, V., Longair, M., Pietzsch, T., Preibisch, S., Rueden, C., Saalfeld, S., Schmid, B., et al. (2012). Fiji: an open-source platform for biological-image analysis. Nat. Methods *9*, 676–682.

Shim, H.G., Lee, Y.S., and Kim, S.J. (2018). The emerging concept of intrinsic plasticity: activity-dependent modulation of intrinsic excitability in cerebellar Purkinje cells and motor learning. Exp. Neurobiol. *27*, 139–154.

Sirec, T., Benarroch, J.M., Buffard, P., Garcia-Ojalvo, J., and Asally, M. (2019). Electrical polarization enables integrative quality control during bacterial differentiation into spores. iScience *16*, 378–389.

Stratford, J.P., Edwards, C.L.A., Ghanshyam, M.J., Malyshev, D., Delise, M.A., Hayashi, Y., and Asally, M. (2019). Electrically induced bacterial membrane-potential dynamics correspond to cellular proliferation capacity. Proc. Natl. Acad. Sci. USA *116*, 9552–9557.

Suh, S., Moran, N., and Lee, Y. (2000). Blue light activates potassium-efflux channels in flexor cells from *Samanea saman* motor organs via two mechanisms. Plant Physiol *123*, 833–843.

Sweatt, J.D. (2016). Neural plasticity and behavior – sixty years of conceptual advances. J. Neurochem. *139*, 179–199.

Tsien, R.Y. (2013). Very long-term memories may be stored in the pattern of holes in the perineuronal net. Proc. Natl. Acad. Sci. USA *110*, 12456–12461.

STAR★METHODS

KEY RESOURCES TABLE

REAGENT or RESOURCE	SOURCE	IDENTIFIER
Bacterial and Virus Strains		
B. subtilis NCIB 3610	Bacillus Genetic Stock Center (Irnov and Winkler, 2010)	BGSCID: 3A1
yugO::neo	(Prindle et al., 2015)	N/A
Software and Algorithms		
Custom MATLAB and Fiji scripts	(Schindelin et al., 2012)	N/A

RESOURCE AVAILABILITY

Lead Contact

Gürol M. Süel, UC San Diego, Pacific Hall Room 2225B, Mail Code 0347, 9500 Gilman Drive, La Jolla, CA 92093, (858) 534-0041, gsuel@ucsd.edu

Materials Availability

Further information and requests for resources and reagents should be directed to and will be fulfilled by the Lead Contact, Gürol M. Süel (gsuel@ucsd.edu). This study did not generate new unique reagents.

Data and Code Availability

This study did not generate new code nor software. All raw data are available upon request from the Lead Contact.

EXPERIMENTAL MODEL AND SUBJECT DETAILS

Bacterial Strains

All experiments were performed using *Bacillus subtilis* NCIB 3610. The wild-type strain was a gift from W. Winkler (University of Maryland) (Irnov and Winkler, 2010). The YugO deletion strain (ΔyugO) was previously described by Prindle et al. (2015).

Growth Conditions

Cells from −80 °C glycerol stock were streaked onto an LB agar plate and incubated at 37 °C overnight. The next morning, a single colony was picked from the plate and inoculated into 3 ml of LB broth and incubated at 37 °C with shaking. After 2.5 h of incubation (OD_{600} ~ 2.3±0.3), the cell culture was centrifuged at 2,100 relative centrifugal force (rcf) for 2 min, and the cell pellet was re-suspended in MSgg (5 mM potassium phosphate buffer (pH 7.0), 100 mM MOPS buffer (pH 7.0, adjusted using NaOH), 2 mM $MgCl_2$, 700 μM $CaCl_2$, 50 μM $MnCl_2$, 100 μM $FeCl_3$, 1 μM $ZnCl_2$, 2 μM thiamine HCl, 0.5% (v/v) glycerol and 0.5% (w/v) monosodium glutamate) and immediately loaded into a commercial Y04D microfluidic plate (EMD Millipore) (Liu et al., 2015). The flow of MSgg was driven by a pump pressure of 1.5 psi. Cells were incubated at 37°C for 90 minutes, and then the temperature was lowered to 30°C for the rest of the experiment. Membrane potential dynamics were measured using the fluorescent cationic dye Thioflavin-T (ThT, Acrosorganics, CAS: 2390-54-7) at a concentration of 10 μM, added after 16-18 h of biofilm growth. In the case of chemical clamp and periodically increased ionic concentration, the ion solution was added into MSgg with 10 μM Thioflavin-T dye, with pressure increased to 3 psi to shorten the time needed to fully replace the regular media. The incubating time with excess cations was always less than 1 h to minimize stress on the biofilm.

METHOD DETAILS

Data Analysis

To calculate percent change in membrane potential indicator ThT and cell death reporter propidium iodide and sytox green (Figures 1E, 1H, S1B, S1C, S2B, and S2D), the background fluorescence was subtracted from all images. Next, we measured the ThT intensity just before exposure and 40 minutes after exposure in both the exposed and unexposed regions. ThT changes for both regions were calculated by subtracting the pre-exposure value from the post-exposure value. In order to obtain the ThT changes caused only by light exposure, the ThT changes in the unexposed region were subtracted from the ThT changes in the exposed region. The resulting value was additionally normalized by dividing by the pre-exposure value in the exposed region. Data in Figure S1A include original ThT intensity with minimum value shifted to 0.

The data in Figures 2E and S1D was calculated by subtracting data of the unexposed region from data of the exposed region, and then normalized such that the value right before exposure corresponds to 0 and the maximum value corresponds to 1.

To calculate correlation coefficients for each time point in Figure 3C, we used the signal intensities of individual pixels at that time point and the signal intensities of the same pixels at time t=0 min. The correlation coefficient is the Pearson correlation coefficient of these two series.

Data in Figures 4D and S4A was first detrended by subtracting the rolling average of 8 consecutive data points to accommodate for any changes in signal intensity due to biofilm growth. The detrended data was checked with the Dickey–Fuller test, which is a standard statistical test for stationarity. Next, the dataset was smoothed with a Savitzky-Golay filter and normalized by min-max normalization. Data in Figure S4B was detrended and smoothed the same way as for Figures 4D and S4A, but without normalization. The y-axis value of processed data was shifted such that the final exposed and unexposed time traces had the same average value as the original time traces.

The methods in other figures with quantitative data not describing here are shown in the legends of those figures.

Experimental Reproducibility

Data shown in the main figures were drawn from a minimum of three independent experiments. For multiple strains or conditions in each figure, such as Figures 1E and 1H, we always performed head-to-head experiments (separate chambers in the same microfluidic device) on the same day to eliminate possible artifacts.

Model Equations and Description

The parameters used in the model are listed in Table S1. As in the model of electrical signaling from Prindle et al. (2015) (Prindle et al., 2015), we describe the dynamics of the membrane potential V of a *B. subtilis* cell as depending on the electric current caused by the flow of potassium ions through potassium ion channels, and by a generic leak current:

$$\frac{dV}{dt} = -g_K n^4 (V - V_K) - g_L (V - V_L) \quad \text{(Equation 1)}$$

The leak Nernst potential V_L is approximated with the following linear function, which increases with increasing extracellular potassium E:

$$V_L = V_{L0} + \delta_L E \quad \text{(Equation 2)}$$

The potassium Nernst potential V_K is given by the following equation:

$$V_K = V_{K0} \ln\left(\frac{E}{I}\right) \quad \text{(Equation 3)}$$

The local extracellular potassium concentration E and intracellular potassium concentration I are modeled explicitly:

$$\frac{dE}{dt} = F g_K n^4 (V - V_K) + (\alpha_K I - \beta_K E) - \gamma_e (E - E_m) \quad \text{(Equation 4)}$$

$$\frac{dI}{dt} = -F g_K n^4 (V - V_K) - (\alpha_K I - \beta_K E) \quad \text{(Equation 5)}$$

Potassium can flow into or out of the cell through the potassium channels (first term on the right-hand side of the above equations) or be actively pumped into or out of the cell (second term). In addition, the local extracellular potassium concentration relaxes to a global extracellular potassium level E_m, which represents the potassium concentration of the media flowing through the chamber as in the models from Martinez-Corral et al. (Martinez-Corral et al., 2019).

The potassium channel is assumed to have four subunits. The dynamics of each subunit are described by the following equation representing the fraction of subunits n that are in the open position, where the first term on the right-hand side of the equation represents the opening of the channels, and the second term represents their closing:

$$\frac{dn}{dt} = \frac{\alpha_0 S}{S_{th} + S}(1 - n) - \beta n \quad \text{(Equation 6)}$$

As described by Prindle et al. (2015) (Prindle et al., 2015), the rate of opening of the channels is assumed to depend on metabolic stress, represented by the variable S, with higher stress causing the channels to open faster. Stress is triggered by changes in membrane potential:

$$\frac{dS}{dt} = \frac{\alpha_s (V_{th} - V)}{exp\left(\frac{V_{th} - V}{\sigma}\right)} - \gamma_s S \quad \text{(Equation 7)}$$

The ThT concentration T is assumed to depend on the difference between a fixed voltage V_0 and the membrane potential V, and to decay at rate γ_t:

$$\frac{dT}{dt} = \alpha_t(V_0 - V) - \gamma_t T \quad \text{(Equation 8)}$$

To model light exposure, we assume that irradiation fixes the subunits of the potassium channels, that is, $\frac{dn}{dt} = 0$ for the light-exposed cells. Thus n is fixed at some constant n_0.

We model a periodic potassium shock by periodically alternating the external potassium parameter E_m between a high value E_{high} and a low value E_{low}. The ThT response of the light-exposed cells is anti-phase to the ThT response of the unexposed cells. The anti-phase behavior of the light-exposed and -unexposed cells relies on three factors:

1. At their equilibrium states, if the extracellular potassium level is low, the unexposed cells have a higher membrane potential than the light-exposed cells.
2. At their equilibrium states, if the extracellular potassium level is high, the unexposed cells have a lower membrane potential than the light-exposed cells.
3. The characteristic response to high extracellular potassium described in Prindle et al. (2015) (Prindle et al., 2015), where a cell depolarizes and then hyperpolarizes in response to a potassium shock, is suppressed in light-exposed cells, which only depolarize.

QUANTIFICATION AND STATISTICAL ANALYSIS

Time-lapse Microscopy

The dynamics of light-exposed biofilms were recorded using an Olympus IX83 inverted epifluorescence microscope with autofocus. 10x /0.3 NA or 40x/0.6 NA objectives were used in the experiments. Biofilm phase contrast and fluorescence images (CFP, 438/24-25 nm, 17 ms exposure) were taken every 10 min, except for the data used in Figures 1D and 1E, where images were taken every 5 min. For high temporal resolution data (Figure S3), images were taken every 10 sec.

Light stimulation was applied with 5 seconds exposure to blue light (438/24-25 nm) through 40x/0.6 NA objectives. The size of the exposed area ($\sim 2\times10^{-8}$ μm^2) was adjusted with an aperture. For experiments that compare membrane potential (ThT) change in different strains or conditions, the intensity of the fluorescent lamp was set to 95 mW (25% maximum intensity). For experiments with periodic external potassium fluctuations, the exposure intensity was set to 190 mW (50% maximum intensity). The pattern in Figures 3A and 3B was encoded using Nikon A1R-HD live cell confocal. Stimulation was performed using 445 nm laser at 75% laser power (maximum output 20 mW), 1 μm per pixel dwell time, 5 repeats. The stimulated biofilm was imaged every 15 minutes.

Image Analysis

Fiji/ImageJ (National Institutes of Health) (Schindelin et al., 2012) and MATLAB (MathWorks) were used for image and data analysis. We generated custom scripts and used the image analysis toolbox to perform image segmentation of fluorescence images.

ADDITIONAL RESOURCES

All relevant resources are contained in the previous STAR Methods sections.